THE JOURNAL OF PHYSICAL CHEMISTRY C

Article

Density Functional Theory Study of the Adsorption of Au Atom on Cerium Oxide: Effect of Low-Coordinated Surface Sites

Norberto J. Castellani, Mari#a M. Branda, Konstantin M. Neyman, and Francesc Illas

J. Phys. Chem. C, **2009**, 113 (12), 4948-4954• DOI: 10.1021/jp8094352 • Publication Date (Web): 05 March 2009

Density Functional Theory Study of the Adsorption of Au Atom on Cerium Oxide: Effect of Low-Coordinated Surface Sites

Norberto J. Castellani,[†,‡] María M. Branda,[†,‡] Konstantin M. Neyman,[§,||] and Francesc Illas*[,§]

Consejo Nacional de Investigaciones Científicas y Tecnológicas, Argentina, Departamento de Física, Universidad Nacional del Sur, 8000 Bahía Blanca, Argentina, Departament de Química Física and Institut de Química Teòrica i Computacional (IQTCUB), Universitat de Barcelona, C/ Martí i Franquès 1, 08028 Barcelona, Spain, and Institució Catalana de Recerca i Estudis Avançats, 08010 Barcelona, Spain

Received: October 24, 2008; Revised Manuscript Received: January 20, 2009

Periodic density functional calculations within the LDA+U and GGA+U formalisms have been carried for slabs representing the $CeO_2(111)$ surface and a stepped model surface. The surface active sites have been determined and the chemical bond between Au and the underlying substrate quantified by means of analysis of Bader charges and calculated magnetic moments. For most of the active sites involving O atoms at (111) terraces or at the corresponding step edges the adsorption energy is very similar (~0.7 eV), and adsorbed Au remains essentially neutral. However, the interaction of Au with one of the facets intersecting the (111) terrace is much stronger (2.4 eV), and the adsorbed metal atom is oxidized. The present results permit one to understand the very large effect of nanostructured ceria on the activity of Au supported catalysts reported recently.

1. Introduction

Stoichiometric (CeO_2) and nonstroichiometric (CeO_{2-x}) cerium oxide, hereafter referred to simply as ceria, is well-known for its oxygen storage capacity and thus has long been used as an active support in supported metal-based catalysts for oxidation reactions.[1] It is believed that ceria can act as an oxygen buffer by releasing/uptaking oxygen through redox processes involving the Ce^{4+}/Ce^{3+} couple, which indeed plays an important role in many oxidation processes, for instance in the three-way catalysts. The reducibility and catalytic activity of CeO_2 are significantly enhanced by the presence of a small amount of transition metals. On the other hand, finely dispersed gold nanoparticles supported on a variety of oxides, ceria among them, have been found to lead to highly active catalyst for many important reactions including CO oxidation, water gas shift reaction (WGS), hydrocarbon oxidation, and NO reduction at low temperatures.[2−17] In particular, nanostructured gold ceria oxidation catalysts have shown to exhibit certain unique properties for low-temperature reformate gas processing. This is the case for the gold ceria catalyst activity toward the WGS reactions, already identified in the first report on this catalytic system,[18] and has since been examined in several other publications concerning a variety of chemical reactions.[19−26]

A very important issue concerning the Au/CeO_x based catalysts is the oxidation state of the Au atoms.[4] Some authors assigned the activity of the Au/CeO_x catalyst in the WGS reaction to the presence of positively charged gold,[7] although it seems also clear that the oxidation state of Au changes with the composition of the gas.[27] The existence of cationic Au on Au/CeO_x catalysts has also been invoked by Guzman et al.[25] and by Pillai and Deevi[28] based on data regarding the CO oxidation reaction. The latter authors assigned the high activity of Au/CeO_x catalysts for CO oxidation to Au^+-OH^- and highly dispersed Au(0) species strongly interacting with defects in the ceria surface. Density functional calculations by Liu et al.[29] for Au on $CeO_2(111)$ slab models also seem to support this assignment. The role of ceria in this case would be to stabilize the cationic $Au^{\delta+}$ species by reducing partially Ce^{4+} cations. However, some other authors suggest that metallic Au nanoparticles, and hence neutral Au atoms, are responsible for the WGS activity at higher temperature.[30,31] In addition, X-ray absorption fine-structure (NEXAFS) spectroscopy studies have shown that, under the typical conditions of the WGS reactions, $Cu^{\delta+}$ and $Au^{\delta+}$ species are not stable.[30,31] Subsequent studies by some of these authors concluded that catalysis is indeed performed by neutral gold and X-ray photoelectron spectroscopy (XPS) data confirmed the lack of oxidation of Cu and Au nanoparticles after the WGS reaction.[32,33]

From the discussion above it is clear that, at present, the electronic/oxidation state of the active site in this system is at least unclear. Theoretical calculations on well defined model systems can shed some light on this intriguing system. There is some claim that Au atoms on stoichiometric $CeO_2(111)$ tend to acquire a noticeable positive charge.[29] However, this conclusion relies on density *functional* calculations using a pure generalized-gradient approach (GGA) exchange-correlation functional. Here, it is important to point out that whereas the description of the insulating CeO_2 within conventional GGA methods is more or less straightforward,[34] to the point that recent DFT calculations represent this material in close accordance with experimental findings and with little dependence on the exchange-correlation functional employed,[34−36] the GGA metallic description of Ce_2O_3, the prototypal reduced ceria system, is simply wrong,[35,36] thus casting reasonable doubts about the conclusions reached about the reduction of Ce atoms by Au adsorption on $CeO_2(111)$ presented by Liu et al.[29]

Clearly, to achieve a physically meaningful and accurate description of ceria systems containing formally Ce^{3+} cations, either because of their stoichiometry or because of the result of some chemical interactions, it is necessary to go beyond LDA and GGA and use an exchange-correlation potential able to

* To whom correspondence should be addressed. E-mail: francesc.illas@ub.edu.
† Consejo Nacional de Investigaciones Científicas y Tecnológicas.
‡ Universidad Nacional del Sur.
§ Universitat de Barcelona.
|| Institució Catalana de Recerca i Estudis Avançats.

10.1021/jp8094352 CCC: $40.75
Published on Web 03/05/2009

account for the localized character of the Ce f electron in the Ce^{3+} oxidation state. There are several ways to repair the shortcomings of standard LDA and GGA: by correcting for the self-interaction error,[37,38] by explicit inclusion of an effective local two-electron one-center repulsion U_{eff} term resulting in the LDA+U or GGA+U approaches,[39−41] or by accounting for nonlocal character of exchange interactions using hybrid DFT approaches.[42,43] Several of these methods have already been applied to the study of cerium oxides and provided a satisfactory description of their electronic structure,[34,44−48] including the somewhat controversial description of oxygen vacancies.[49]

Ceria is no doubt a very complex system, and up to date the only results which may be claimed to approach ab initio quality are those relying on the application of hybrid approaches as shown initially by Hay et al.[47] in their study of bulk CeO_2 and Ce_2O_3 using Gaussian type orbitals and later by Da Silva et al.[48] using a planewave basis set. Nevertheless, one has to realize that hybrid DFT is not free of problems because the amount of Fock exchange included in the potential is also an external input which largely affects the final description.[50,51] In any case, the work of Loschen et al.[34] shows that the description of bulk CeO_2 and Ce_2O_3 reached by LDA+U and GGA+U is very close to that obtained from hybrid DFT calculation.[47,48] Thus, LDA+U and GGA+U offer a good compromise between accuracy and computational cost. In this work we use these methods to study the interaction of Au with two different types of CeO_2 surfaces. These are the CeO_2(111) ideal surface and a model including steps and, hence, allowing one to investigate the effect of low-coordinated surface sites while preserving the chemical stoichiometry.

2. Computational Details

In this work, periodic LDA+U and GGA+U calculations have been carried out for a series of slab models representing the ideal CeO_2(111) surface and a model introducing low coordinated sites taken from a recent work on stepped CeO_2 surfaces.[52] The method has been described at length in the original papers[39−41] and also in recent work concerning precisely the stepped surfaces.[52] Consequently, here we will only mention that we are using the formalism due to Dudarev et al.[53] which makes use of a single U_{eff} (hereafter simply denoted as U) parameter. A key point is the choice of U since it determines to a large extent the final results. Thus, our choice comes from the systematic study by Loschen et al.[34] where this parameter has been taken as semiempirical and adjusted to simultaneously reproduce several experimental observables for bulk CeO_2 and Ce_2O_3. These are lattice parameter, band gap, and formation energies of both oxides plus proper antiferromagnetic ground state, magnetic moment and 4f degree of localization density on the Ce^{3+} cations of Ce_2O_3. In addition, this choice seems to be able to properly describe localization in ceria nanoparticles containing both Ce^{3+} and Ce^{4+} atoms.[54−56] Indeed, the optimum value of U thus obtained is different for LDA and GGA. Thus, LDA+U and GGA+U have been used with U values of U = 5 eV for LDA+U and U = 3 eV for GGA+U with the VWN[57] and PW91 exchange-correlation potential[58,59] for the LDA and GGA part, respectively. The smaller U value for GGA+U has been attributed to the more accurate treatment of correlation effects within the GGA potential. This is because the U term does not represent the electronic correlation of two electrons in one center but the difference between the LDA or GGA representation of this electron−electron correlation and the exact value, the latter being unknown and hence taken by comparison to experiment.[60] Note, however, that for CeO_2 there is clear indication that structural properties such as lattice constants and bulk modulus are somewhat better represented by the LDA+U method, whereas for Ce_2O_3 both LDA+U and GGA+U results show a similarly good accuracy. The GGA lattice parameter of CeO_2 is overestimated (5.48 Å, while the experimental value is of 5.41 Å) and increases with U. For Ce_2O_3, the LDA lattice parameter is underestimated but increases with U and reaches the experimental value for U = 3 eV. Therefore, one faces the following dilemma: to use the GGA+U results for geometry and energy, which is usually the preferred approach, even knowing that this leads to a somewhat expanded lattice and consequent risk of a biased description toward reduced Ce (which is larger than Ce^{4+}) induced by Au or to use the LDA+U geometry, which is closer to experiment, and to estimate the energy and density from GGA+U, which provides a more accurate description than LDA+U for energy data. We followed the latter option which is also the strategy used in previous work[52] and carried out geometry optimization at the LDA+U level, whereas energies, charges, and magnetic moments have been calculated by a GGA(PW91)+U approach. Following the notation often used for quantum chemical calculation, we will hereafter refer to this procedure as GGA//LDA. The combined GGA//LDA strategy has been justified for calculations of 4D-metal particles[61] based on the observation that GGA for chemical bonds of heavy elements usually only improves energy values but makes geometries less accurate.[62] This procedure may seem inadequate because one may argue that the structure is not an energy minimum for the functional used to compute the energy. However, it is clear that the alternative may lead to biased results because the minimum energy structure consistent with the functional is rather far from experiment. Unfortunately, there is no rigorous way to decide among the two possible options and we have taken the most pragmatic approach. This issue is nevertheless important and deserves perhaps a more systematic study which is beyond the scope of the present work.

To investigate the oxidation state of adsorbed Au and underlying Ce atoms net charges have been calculated using the topologic Bader analysis[63] using the GGA+U density. This procedure is more accurate than integration of the electron density in a given volume since it permits one to take into account the changes in atomic volume accompanying a change in oxidation state. In fact, it has been recently shown that calculated net charges on a given fixed volume can appear to be independent of the oxidation state.[64] This is not the case for charges calculated following the Bader analysis. In fact, for bulk CeO_2 and Ce_2O_3 the Bader charge on Ce atoms is +2.4 and +2.0 e, respectively, and for the latter one finds also a magnetic moment of 0.96 μ_B resulting from the localized 4f electron in Ce^{3+}. The combined use of calculated Bader charges and magnetic moments permits one to firmly establish the oxidation state of Au and Ce atoms in the Au on CeO_2 models studied in the present work and to clearly identify two types of Ce atoms in the different surface models here explored.

All calculations have been carried out with the Vienna ab initio simulation package (VASP).[65,66] The valence electronic states were expanded in a basis of plane waves with a cutoff of 415 eV for the kinetic energy and the effect of the core electrons on the valence states was represented with the projector augmented wave (PAW) approach[67] as implemented in VASP.[68] The total energy threshold defining self-consistency of the electron density was set to 10^{-4} eV, and the convergence criterion for structural optimization was set to be a total energy difference less than 10^{-2} eV for consecutive geometries. Optimized geometries were then refined until forces on atoms

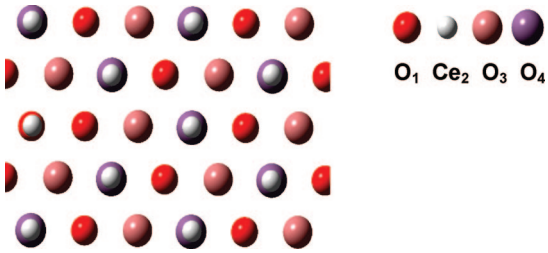

Figure 1. Schematic top representation of the $CeO_2(111)$ surface model used. The Au adsorption sites are on-top over O_1, Ce_2, and O_3.

were smaller than 0.01 eV/Å^2 and characterized as minimum energy stationary points by proper analysis of the vibrational frequencies involving the Au atom. Numerical integration in the reciprocal space was carried out using a sufficiently dense grid of Monkhorst-Pack special k points.[69] The specific grids used for each surface model are discussed in the next section below.

3. Surface Models

A slab model containing six atomic layers (Figure 1) was first constructed for the perfect, O-terminated, $CeO_2(111)$ surface with a vacuum width of ~12 Å between the neighboring interleaved slabs. The slab was cut from the bulk cubic (Fm3m) CaF_2 structure using the optimized lattice parameter value a_0 of 5.39 Å as obtained from LDA+U calculation with $U = 5$ eV.[34] Note that this is in excellent agreement with the experimental available results of $a_0 \approx 5.41$ Å (5.406(1) Å[70] or 5.411(1) Å[71]). Previous work with slab models containing up to 15 atomic layers has shown that a slab with 9 layers with the 6 uppermost layers fully relaxed provides nearly converged results and only the three uppermost layers exhibit a significant relaxation. Therefore, a slab with six atomic layers should be appropriate to study the adsorption of atomic Au with this ideal surface. In fact, the atomic displacements of the three uppermost layers in the 6 and 9 layers slab models is practically identical thus predicting a very similar surface relaxation. To maximize the Au−Au distances, a Ce_8O_{16} 2 × 2 supercell has been used which eventually contains also 1 Au atom above selected surface sites. For this unit cell a 4 × 4 × 1 grid of special k points was used.

To investigate the interaction of Au with low coordinated sites while maintaining the CeO_2 stoichiometry a slab model has been constructed following the strategy outlined in a previous recent work.[52] This starts from a $Ce_{16}O_{32}$ 4 × 2 supercell for the CeO2(111) surface and generates a stepped surface by removing from this unit cell two CeO_2 structural units, thus resulting in $Ce_{14}O_{28}$. This is done in such a way that one O row in the *y* direction in the topmost atomic layer (Figure 2) and the subsequent Ce and O rows in the second and third atomic layers are removed, thus resulting in a stoichiometric slab model with a $Ce_{14}O_{28}$ formula unit and containing one (111) terrace and with the lateral surfaces of the strip perpendicular to the ⟨111⟩ direction corresponding to (−211) or (11−2) Miller planes. For the resulting model, full relaxation of the atomic positions was allowed by maintaining fixed the three bottom ones. This model is found to be stable with important atomic displacements from the original geometry. In addition, the displacements are very similar to those found for a similar model containing 9 atomic layers.[52]

4. Results and Discussion

A. Au on the Perfect $CeO_2(111)$ Surface. For the interaction of Au with the $CeO_2(111)$ surface various surface sites have been considered but after full geometry optimization converged to three unique situations that have been characterized as energy minima with respect to the displacement of the Au atom in any direction. These correspond to the interaction of the Au atom directly on top of an oxygen atom on the first atomic layer (O_1), the interaction of Au above an oxygen atom of the third atomic layer, and, hence, coordinated to three Ce atoms on the second layer (O_3) and directly above a Ce atom on the second atomic layer (Ce_2), and, therefore, coordinated to three O atoms of the first atomic layer. Table 1 reports a summary of the most important geometric and electronic parameters and evidence that the most favorable site corresponds to the interaction above the O_1 site. In addition, analysis of the structure of the surface after Au deposition does not evidence any noticeable additional relaxation. The prediction for the most stable site and the present GGA+U ($U = 3$ eV) technique gives an adsorption energy value of 0.66 eV that is close to the 0.88 GGA+U ($U = 5$ eV) one reported recently by Chen et al.[72] using the same type of computational setup although with a ticker slab with 9 atomic layers and a somehow larger cutoff for the kinetic energy. In any case, the 0.22 eV energy difference is likely to be mainly due to the difference in the *U* value. Note, also, that the present value for the Au−O_1 distance (207 pm) is closest to the GGA+U value of Chen et al. (211 pm). These authors also report adsorption energies of 0.63 and 0.79 eV calculated using localized basis sets and the BLYP and GGA functionals and Au−O_1 distances of 218 pm. Therefore, one can conclude that a reasonable estimate of the adsorption energy of Au on $CeO_2(111)$ is 0.77 ± 0.11 eV. This value is considerably smaller that the estimate of 1.26 eV reported by Liu et al.[29] obtained by using the PBE implementation of the GGA exchange-correlation functional. The difference between this and the rest of adsorption energy values commented above is likely to be due to the use of ultrasoft pseudopotentials to describe the core electrons and, perhaps, a too small value of the cutoff energy. Nevertheless, it is important to point out that Liu et al.[29] also predict O_1 to be the most active site for the interaction of Au on $CeO_2(111)$.

The next important issue concerns the degree of charge transfer between Au and the $CeO_2(111)$ surface. The net charge on Au calculated by the Bader atoms in molecules analysis using the GGA+U ($U = 3$ eV) density is −0.02 e and, hence, qualitatively different from the +0.35e value reported by Liu et al.[29] The absence of atomic charge in the Au is consistent with the existence of a magnetic moment of 0.35 μ_B on the Au atom, estimated from the integration of the spin density in the volume defined by the atomic radius, and the absence of any noticeable magnetic moment on the Ce ($\mu_{Ce} < 0.10\ \mu_B$) atoms. Clearly, the present GGA+U calculations do not support the claim by Liu et al.[29] that the interaction of Au atoms with $CeO_2(111)$ results in a charge transfer from Au to the oxide substrate resulting in an adsorbed cationic $Au^{\delta+}$ species. In principle one may think that the charge transfer from the Au (6s) to the Ce(4f) orbital is an artifact of the exceedingly low O(2p)-Ce(4f) gap predicted the GGA functional. In fact, the calculated value with $U = 0$ eV is of ~1.3 eV, while the experimental value is of 3 eV. Including the *U* term in the Ce(4f) manifold results in a larger O(2p)-Ce(4f), which is of ~1.8 eV for $U = 3$ eV. Therefore, one may argue that the too small value of the O(2p)-Ce(4f) gap has undesired consequences; the Ce(4f) levels appear close to the Au(6s), and as a consequence, the Au (6s) electron density would be transferred to the Ce(4f) levels. To verify this hypothesis, calculations have been carried out using the same computational approach but using GGA

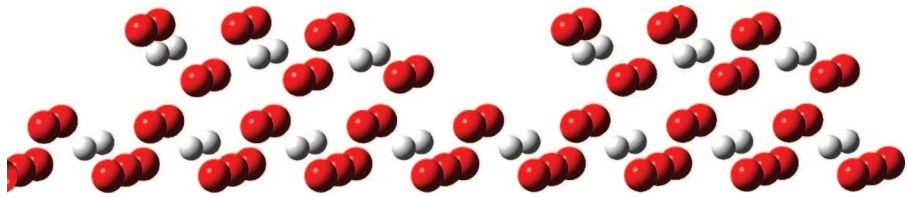

Figure 2. Schematic representation of the relaxed 4 × 2 $Ce_{14}O_{28}$ unit cell model of the stepped surface.

TABLE 1: Relevant Data for the Interaction of Au on CeO_2(111) as Predicted from GGA+U (U = 3 eV) Calculations[a]

	surface site		
	O_1	O_3	Ce_2
E_{ads} (kJ mol^{-1})	63.7	49.2	33.8
E_{ads} (eV)	0.66	0.51	0.35
d_{Au-O} (pm)	207	259	300
q_{Au}	−0.02	−0.01	−0.01
μ_{Au} (μ_B)	0.31	0.26	0.37

[a] E_{ads} stands for the adsorption energy with respect to the isolated Au and the naked slab model; d_{Au-O} corresponds to the distance between Au and the nearest surface O atoms; q_{Au} is the Bader net charge on adsorbed Au; μ_{Au} its corresponding magnetic moment.

instead of GGA+U. The adsorption energy becomes 0.73 eV, closer to the BLYP and GGA values reported by Chen et al.[72] However, the calculated Bader charge and magnetic moment on the adsorbed Au atom are only slightly changed, the GGA values being q_{Au} = +0.01 e and μ_{Au} = 0.35 μ_B, indicating some weak tendency toward Au oxidation but far from the large positive charge and zero magnetic moment predicted by the DFT calculations of Liu et al.[29] obtained by using a very similar computational approach. Additional calculations were carried out starting from different types of spin-polarized solutions but the self-consistent field always converged to the same solution. This is the case even when the starting density corresponds to a reduced Ce^{3+} atom and an oxidized Au^+ atom. To the extent that DFT permits to control the spin symmetry,[73] the multiplicity was also analyzed, but it was found that the lower total energy corresponds to a doublet state with one unpaired electron. At this point it is very difficult to understand the origin of the difference in the oxidation state of Au adsorbed on the stoichiometric CeO_2(111) predicted by the present and previous calculations, the only noticeable difference between the two calculations being the description of the electron cores, ultrasoft pseudopotentials in the work of Liu et al.[29] vs PAW here. Comparison to the previous work of Chen et al.[72] could help to solve this puzzle; we already mentioned that the most stable site, structural data, and the adsorption energy values are close to those reported in Table 1, but unfortunately, these authors do not report atomic charges on the Au atom, and hence, further comparison is unattainable.

Before closing this subsection we would like to comment on results from two recent works concerning the interaction of metal atoms with the regular sites of the CeO_2(111) surface.[74,75] These works consider Pd[74] and Au[75] atoms, respectively, and find a noticeable degree of charge transfer between the metal and the surface. In the case of Pd one has to note that it is less electronegative (2.20, Pauling scale) than the Au atom (2.54, Pauling scale). Thus, the formation of a cationic adsorbed atomic $Pd^{\delta+}$ species on CeO_2(111) would not necessarily mean formation under similar conditions of adsorbed atomic $Au^{\delta+}$ species. Also, these authors find that the adsorption energy at the site with charge transfer (−1.91 eV) is not that far from the one corresponding to the "no charge transfer" site (−1.75 eV). Here, one must point out that the authors use a GGA+U with U = 5 eV and the corresponding lattice parameter. We already commented that the use of this somewhat expanded geometry may bias the results toward reduced ceria simply because it allows the extra space needed to accommodate the Ce^{3+} cation. This will explain the present result that increasing U up to 5 eV does not lead to Au^+ when using the LDA+U geometry, which is very close to the experimental value. Nevertheless, previous results strongly suggest that a value of U = 5 eV for the GGA+U calculations is probably too high.[34] Another important aspect concerns the relative stability of the two sites as a function of the U value. The same caveat applies to the results of Zhang et al. for Au on the regular sites of CeO_2(111).[75] These authors also use the energy arising from GGA+U (U = 5 eV) and the corresponding geometry. By use of the same procedure we fully reproduce their results, confirming that they are induced by the simultaneous use of a lattice parameter larger than the experimental one and a too large U value. At this point it is clear that a systematic study exploring the effect of lattice parameter and of the choice of U on the redox properties of ceria is needed.

B. Au on the a Stepped Surface Model of CeO_2. The stepped surface model described in the previous section is similar to most stable of the step models described in a recent work;[52] it is stoichiometric and contains (111) terraces and also (−211) or (11−2) planes, hereafter referred to as concave and convex, which can be clearly identified in Figure 2. A first important point concerns the structural stability of the model; geometry optimization preserves mostly the original topology although interatomic distances are noticeably changed with respect to the bulk values (±20 pm) due to the presence of low coordinated sites. Indeed, the final geometry is very similar to that reported in previous work in spite of the fact that the present model reveals smaller distance between the separated (111) terraces. Several adsorption sites for Au were considered on the (111) terraces as well as on the concave and convex facets. However, after geometry relaxation only six stable adsorption sites were found, all characterized as minima by proper vibrational frequency analysis. Three of these sites correspond to the direct interaction of Au with surface O atoms of the (111) terrace and are denoted as S1, S2a, and S2b, respectively. S1 corresponds to the most inner O atoms of the terrace and S2a and S2b to O atoms in the step edge. The only difference between S2a and S2b is the tilting of the Au atoms either toward the terrace or to the open space nearby (Figure 3a). The three remaining sites involve coordination of Au to various surface O atoms. Thus, S3 involves a 2-fold interaction with one O surface atom at the step edge and one O atom in the fourth atomic layer in the concave facet. Finally, S4 and S5 are 3-fold sites in the (111) terrace but involving O atoms at the step edge either near the concave or convex facets (Figure 3b).

For the S1, S2a, and S2b sites, the adsorption energy is very close to that obtained for the interaction of Au with the surface O atoms of the CeO_2(111) perfect terrace. In fact, for the S1 site, the adsorption energy is identical to that corresponding to the O1 site of the CeO_2(111) terrace, the effect of low

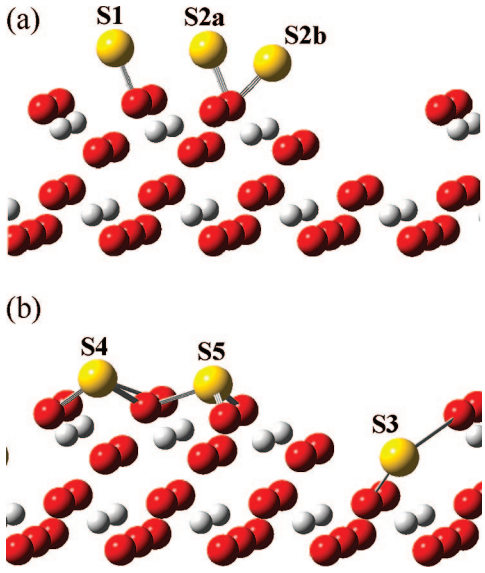

Figure 3. Adsorption sites for Au on the relaxed 4 × 2 $Ce_{14}O_{28}$ unit cell model of the stepped surface. (a) 1-fold sites, (b) 2- and 3-fold sites.

TABLE 2: Relevant Structural Data for the Interaction of Au on the CeO_2 stepped model as predicted from GGA+U (U = 3 eV) Calculations[a]

	surface site					
	S1	S2a	S2b	S3	S4	S5
E_{ads} (kJ mol^{-1})	63.7	66.6	66.6	227.7	65.6	50.2
E_{ads} (eV)	0.66	0.69	0.69	2.36	0.68	0.52
d_{Au-O} (pm)	213	210	212	196	217	276
				201	289	248
					289	248
α (deg)	33	26	47			
q_{Au}	−0.05	−0.03	−0.06	+0.32	+0.02	+0.02
μ_{Au} (μ_B)	0.35	0.32	0.35	0.00	0.27	0.26

[a] E_{ads} stands for the adsorption energy with respect to the isolated Au and the naked slab model; d_{Au-O} corresponds to the distance (S1, S2a, S2b) or nonequivalent distances (S3, S4, S5) between Au and the nearest surface O atoms; α corresponds to the tilting angle respect to the perpendicular direction; q_{Au} is the Bader net charge on adsorbed Au; μ_{Au} its corresponding magnetic moment.

coordination in the S2a and S2b does only increase the adsorption energy by a modest 0.03 eV amount. Not surprisingly, the calculated Bader charge on the adsorbed Au atoms and the corresponding magnetic moment (Table 2) are also almost identical to those reported in Table 1 for the most stable terrace site. Hence, the presence of low-coordinated surface O atoms does not change the nature of the interaction. A similar situation occurs for the 3-fold S4 and S5 sites; the adsorption energy is again close to the value calculated for the most stable terrace site and the calculated Bader charge and magnetic moment on the adsorbed Au do not evidence any tendency that this becomes oxidized. Hence, one can conclude that the interaction of Au atoms with low-coordinated O atoms at the step edge of CeO_2 stepped surfaces is moderately strong and with Au neutral as on the regular CeO_2(111) surface.

A completely different situation is found for the S3 site where the Au atoms interact with the concave facet in one of sides of the step. Here, the interaction energy is much large, 2.36 eV compared to ∼0.70 eV for the remaining sites involving regular or low-coordinated surface O atoms. This strong interaction involves Au and one O atoms at the step edge and one O atom in the fourth layer. Since only the three outermost layers of this model have been fully relaxed one may wonder whether the resulting interaction is an artifact arising from the excessive rigidity of the model. To rule out this possibility, calculations have also been carried out allowing full relaxation of the O atom in the fourth atomic layer directly interaction with Au, the final adsorption energy is only slightly changed becoming 2.41 eV, and the atomic structure is almost unaffected. The difference between adsorption energy at this site and at all other sites characterized as energy minima is so large that one can firmly establish that, for ceria samples containing step edges with facets morphologically similar to those represented by the stepped surface model in Figure 2, interaction of Au atoms will occur only at S3-like sites and other sites could be occupied only for a sufficiently large Au coverage. The larger interaction at the S3 sites is accompanied by a completely different type of chemical bonding. Here, both the large and positive Bader net charge (0.32 e) and the zero calculated magnetic moment at the Au atoms are indicative of a charge transfer between Au and the surface substrate. Further analysis reveals that the charge transfer involves essentially one of the Ce atoms close to Au which indeed becomes oxidized. The charge-transfer mechanism is essentially the same predicted by Liu et al. with the important difference that the present calculations do not find any evidence of this process when Au interacts with either regular terrace O sites or with low coordinated O atoms at the step edges. However, the present results permit one to understand the effect of nanostructured ceria observed by Guzman et al.[25] In fact, nanostructured ceria is likely to present a variety of stepped surfaces and different facets. The interaction of Au with some of these facets results in cationic $Au^{\delta+}$, while the interaction with facets resembling CeO_2(111) likely leads to neutral adsorbed Au. This effect is difficult to understand from model calculations already predicting adsorbed cationic Au at the regular sites of stoichiometric CeO_2(111).

5. Conclusions

The interaction of Au atoms with regular and low-coordinated sites of CeO_2 has been studied by means of periodic density functional calculations within the LDA+U and GGA+U approaches using suitable slab models.

For the regular, O-terminated CeO_2(111) surface, present calculations predict three stable adsorption sites although the most favorable one corresponds to a direct interaction between Au and surface O atoms in the first atomic layers. In all cases, the analysis of Bader charges and of the calculated magnetic moments on adsorbed Au indicates that Au maintains essentially its atomic configuration with no noticeable charge transfer from the adsorbate to the substrate in full agreement with several new experimental results.[30−33] This is in unambiguous conflict with previous calculations using a similar periodic approach and a similar GGA (without U) exchange-correlation potential.[29] The difference also affects the adsorption energy; for the most stable site the present calculations predict a value of 0.66 eV, in good agreement with recent calculations by Chen et al.[72] but much smaller than the result of Liu et al.[29] (1.26 eV), where oxidation of Au is also manifested. Present calculations with U = 0 do not evidence any noticeable charge transfer, and therefore, the origin of these differences remains unclear. It is also important to note that calculations carried out with a larger U value and a more expanded lattice find that Au is most stable on a bridge position with an adsorption energy of −1.17 and with a positive charge on the adsorbate which becomes almost Au^+ but followed by adsorption on-top of an O site with adsorption energy of −0.96 eV and a Bader charge of +0.17 e only.[75] At

this point it is very difficult to decide which of the two descriptions is closest to physical reality and call for a more systematic study including perhaps hybrid density functional theory calculations.

For the stepped surface model six active sites are found among which five involve O atoms either at terrace sites or at the step edges. Interestingly, the interaction of Au with these surface sites is almost the same in spite of the fact that some of the sites involve low-coordinated O atoms. In all these cases, adsorbed Au remains neutral maintaining its unpaired electron. The remaining site involves one of the facets intersecting the (111) terraces. In this case, the interaction of Au is much stronger; the adsorption energy becomes almost four times larger than for the rest of stable sites meaning that, if available, Au will preferentially occupy these sites. In addition, this strong interaction is accompanied by a clear oxidation of the adsorbed Au adatom.

Even if from the present study and the recent literature[75] it is not possible to firmly conclude whether Au becomes oxidized at the regular sites of the $CeO_2(111)$ surface, it is clear that Au oxidation is facilitated at some particular sites of stepped CeO_2 surfaces. The fact that Au oxidation at this site is predicted even by using a U value of 3 eV only strongly supports this conclusion.

The present results permit to explain, at least in part, the observations by Guzman et al.[25] of a larger activity of Au supported on nanostructured CeO_2 catalysts. Nanostructured ceria is likely to exhibit a variety of different facets, and Au oxidation takes place preferentially in some of them. The present results also support the existence of cationic Au in the Au/CeO_2 catalysts explored by Fu et al.[7] although do not support the existence of cationic Au at the regular $CeO_2(111)$ terrace sites. Finally, present results are in full agreement with recent experimental work carried out on well-ordered ceria films showing that the majority of particles nucleate on the step edges[76] and that eventual sintering of Au articles also proceeds mainly along the step edged of the $CeO_2(111)$ support.[77]

Acknowledgment. N.J.C. is grateful to CONICET-Argentina for making possible his stay at the Universitat de Barcelona. This study has been supported by the Spanish Ministry of Education and Science (Grant Nos. CTQ2005-08459-CO2-01, UNBA05-33-001, HA2006-0102), by the Generalitat de Catalunya (Grant Nos. 2005SGR00697 and 2005 PEIR 0051/69), and by the COST-D41 action. Computational time on the MareNostrum supercomputer of the Barcelona Supercomputing Center is gratefully acknowledged.

References and Notes

(1) Trovarelli, A. *Catalysis by Ceria and Related Materials*; Imperial College Press: London, 2002.
(2) Weststrate, C. J.; Resta, A.; Westerstro1m, R.; Lundgren, E.; Mikkelsen, A.; Andersen, J. N. *J. Phys. Chem. C* **2008**, *112*, 6900.
(3) Chen, M. S.; Goodman, D. W. *Science* **2004**, *306*, 252.
(4) Hashmi, A.S. K.; Hutchings, G. J. *Angew. Chem., Int. Ed.* **2006**, *45*, 7895.
(5) Haruta, M.; Kobayashi, Y.; Sano, H.; Yamada, N. *Chem. Lett.* **1987**, *16* (2), 405.
(6) Haruta, M.; Yamada, N.; Kobayashi, T.; Iijima, S. *J. Catal.* **1989**, *115*, 301.
(7) Fu, Q.; Saltsburg, H.; Flytzani-Stephanopoulos, M. *Science* **2003**, *301*, 935.
(8) Haruta, M. *J. Catal.* **1997**, *36*, 153.
(9) Ueda, A.; Oshima, T.; Haruta, M. *Appl. Catal. B* **1997**, *12*, 81.
(10) Blick, K.; Mitrelias, T. D.; Hargreaves, J. S. J.; Hutchings, G. J.; Joyner, R. W.; Kiely, C. J.; Wagner, F. E. *Catal. Lett.* **1998**, *50*, 211.
(11) Fu, Q.; Kudriavtseva, S.; Saltsburg, H.; Flytzani-Stephanopoulos, M. *Chem. Eng. J.* **2003**, *93*, 41.
(12) Burch, R. *Phys. Chem. Chem. Phys.* **2006**, *8*, 5483.
(13) Tabakova, T.; Boccuzzi, F.; Manzoli, M.; Sobczak, J. W.; Idakiev, V.; Andreeva, D. *Appl. Catal. A* **2006**, *298*, 127.
(14) Denkwitz, Y.; Karpenko, A.; Plzak, V.; Leppelt, R.; Schumacher, B.; Behm, R. J. *J. Catal.* **2007**, *246*, 74.
(15) Panzera, G.; Modafferi, V.; Candamano, S.; Donato, A.; Frusteri, F.; Antonucci, P. L. *J. Power Sources* **2004**, *135*, 177.
(16) Luengnaruemitchai, A.; Osuwan, S.; Gulari, E. *Int. J. Hydrogen Energy* **2004**, *29*, 429.
(17) Deng, W.; De Jesus, J.; Saltsburg, H.; Flytzani-Stephanopoulos, M. *Appl. Catal., A* **2005**, *291*, 126.
(18) Fu, Q.; Weber, A.; Flytzani-Stephanopoulos, M. *Catal. Lett.* **2001**, *77*, 87.
(19) Fu, Q.; Deng, W.; Saltsburg, H.; Flytzani-Stephanopoulos, M. *Appl. Catal., B* **2005**, *56*, 57.
(20) Andreeva, D.; Idakiev, V.; Tabakova, T.; Ilieva, L.; Falaras, P.; Bourlinos, A.; Travlos, A. *Catal. Today* **2002**, *72*, 51.
(21) Tabakova, T.; Boccuzzi, F.; Manzoli, M.; Andreeva, D. *Appl. Catal., A* **2003**, *252*, 385.
(22) Luengnaruemitchai, A.; Osuwan, S.; Gulari, E. *Catal. Commun.* **2003**, *4*, 215.
(23) Tabakova, T.; Boccuzzi, F.; Manzoli, M.; Sobczak, J. W.; Idakiev, V.; Andreeva, D. *Appl. Catal., B* **2004**, *49*, 73.
(24) Sakurai, H.; Akita, T.; Tsubota, S.; Kiuchi, M.; Haruta, M. *Appl. Catal., A* **2005**, *291*, 179.
(25) Guzman, J.; Carrettin, S.; Fierro-Gonzalez, J. C.; Hao, Y.; Gates, B. C.; Corma, A. *Angew. Chem., Int. Ed.* **2005**, *44*, 4778.
(26) Si, R.; Flytzani-Stephanopoulos, M. *Angew. Chem., Int. Ed.* **2008**, *47*, 2884.
(27) Deng, W.; Frenkel, A. I.; Si, R.; Flytzani-Stephanopoulos, M. *J. Phys. Chem. C* **2008**, *112*, 12834.
(28) Pillai, U. R.; Deevi, S. *Appl. Catal., A* **2006**, *299*, 266.
(29) Liu, Z. P.; Jenkins, S. J.; King, D. A. *Phys. Rev. Lett.* **2005**, *94*, 196102.
(30) Wang, X.; Rodriguez, J. A.; Hanson, J. C.; Perez, M.; Evans, J. *J. Chem. Phys.* **2005**, *123*, 221101.
(31) Wang, X.; Rodriguez, J. A.; Hanson, J. C; Gamarra, D.; Martinez-Arias, A.; Fernandez; García, M. *J. Phys. Chem. B* **2006**, *110*, 428.
(32) Rodriguez, J. A.; Wang, X.; Liu, P.; Wen, W.; Hanson, J. C.; Hrbek, J.; Perez, M.; Evans, J. *Top. Catal.* **2007**, *44*, 73.
(33) Rodriguez, J. A.; Liu, P.; Hrbek, J.; Evans, J.; Pérez, M. Angew. Chem., Int. Ed. **2008**, (DOI: 10.1002).
(34) Loschen, C.; Carrasco, J.; Neyman, K. M.; Illas, F. *Phys. Rev. B* **2007**, *75*, 035115.
(35) Fabris, S.; de Gironcoli, S.; Baroni, S.; Vicario, G.; Balducci, G. *Phys. Rev. B* **2005**, *71*, 041102.
(36) Kresse, G.; Blaha, P.; Da Silva, J. L. F.; Ganduglia-Pirovano, M. V. *Phys. Rev. B* **2005**, *72*, 237101.
(37) Petit, L.; Svane, A.; Szotek, Z.; Temmerman, W. M. *Phys. Rev. B* **2005**, *72*, 205118.
(38) Gerward, L.; Olsen, J. S.; Petit, L.; Vaitheeswaran, G.; Kanchana, V.; Svane, A. *J. Alloys Compd.* **2005**, *400*, 56.
(39) Anisimov, V. I.; Aryasetiawan, F.; Lichtenstein, A. I. *J. Phys.: Condens. Matter* **1997**, *9*, 767.
(40) Anisimov, V. I.; Solovyev, I. V.; Korotin, M. A.; Czyzyk, M. T.; Sawatzky, G. A. *Phys. Rev. B* **1993**, *48*, 16929.
(41) Solovyev, I. V.; Dederichs, P. H.; Anisimov, V. I. *Phys. Rev. B* **1994**, *50*, 16861.
(42) Becke, A. D. *J. Chem. Phys.* **1993**, *98*, 1372.
(43) Becke, A. D. *Phys. Rev. A* **1988**, *38*, 3098.
(44) Svane, A.; Temmerman, W.; Szotek, Z. *Phys. Rev. B* **1999**, *59*, 7888.
(45) Castleton, C. W. M.; Kullgren, J.; Hermansson, K. *J. Chem. Phys.* **2007**, *127*, 244704.
(46) Jiang, Y.; Adams, J. B.; van Schilfgaarde, M. *J. Chem. Phys.* **2005**, *123*, 064701.
(47) Hay, P. J.; Martin, R. L.; Uddin, J.; Scuseria, G. E. *J. Chem. Phys.* **2006**, *125*, 034712.
(48) Da Silva, J. L. F.; Ganduglia-Pirovano, M. V.; Sauer, J.; Bayer, V.; Kresse, G. *Phys. Rev. B,* **2007**, *75*, 045121.
(49) Ganduglia-Pirovano, M. V.; Da Silva, J. L. F.; Sauer, J. *Phys. Rev. Lett.* **2009**, *102*, 026101.
(50) Martin, R. L.; Illas, F. *Phys. Rev. Lett.* **1997**, *79*, 1539.
(51) Moreira, I. De P.R.; Illas, F.; Martin, R. L. *Phys. Rev. B.* **2002**, *65*, 155102.
(52) Branda, M. M.; Loschen, C.; Neyman, K. M.; Illas, F. *J. Phys. Chem. C* **2008**, *112*, 17643.
(53) Dudarev, S. L.; Botton, G. A.; Savrasov, S. Y.; Humphreys, C. J.; Sutton, A. P. *Phys. Rev. B,* **1998**, *57*, 1505.
(54) Loschen, C.; Bromley, S. T.; Neyman, K. M.; Illas, F. *J. Phys. Chem. C* **2007**, *111*, 10142.
(55) Loschen, C.; Migani, A.; Bromley, S. T.; Illas, F.; Neyman, K. M. *Phys. Chem. Chem. Phys.* **2008**, *10*, 5730.

(56) Migani, A.; Loschen, C.; Illas, F.; Neyman, K. M. *Chem. Phys. Lett.* **2008**, *465*, 106.
(57) Vosko, S. H.; Wilk, L.; Nusair, M. *Can. J. Phys* **1980**, *58*, 1200.
(58) Perdew, J. P.; Chevary, J. A.; Vosko, S. H.; Jackson, K. A.; Pederson, M. R.; Singh, D. J.; Fiolhais, C. *Phys. Rev. B* **1992**, *46*, 6671.
(59) Perdew, J. P.; Chevary, J. A.; Vosko, S. H.; Jackson, K. A.; Pederson, M. R.; Singh, D. J.; Fiolhais, C. *Phys. Rev. B* **1993**, *48*, 4978.
(60) Rivero, P.; Loschen, C.; Moreira, I. de P.R.; Illas, F. *J. Comput. Chem.* **2009**, *30*, 2559.
(61) Yudanov, I. V.; Sahnoun, R.; Neyman, K. M.; Rösch, N. *J. Chem. Phys.* **2002**, *117*, 9887.
(62) Görling, A.; Trickey, S. B.; Gisdakis, P.; Rösch, N. *Topics in Organometallic Chemistry*; Brown, J., Hofmann, P., Eds.; Springer: Heidelberg, 1999; Vol. 4, p. 109
(63) Bader, R. F. W. *Atoms in Molecules: A Quantum Theory*; Oxford Science: Oxford, UK, 1990.
(64) Raebiger, H.; Lany, S.; Zunger, A. *Nature* **2008**, *453*, 763.
(65) Kresse, G.; Hafner, J. *Phys. Rev. B* **1993**, *47*, 558.
(66) Kresse, G.; Furthmüller, J. *Phys. Rev. B* **1996**, *54*, 11169.
(67) Blöchl, P. E. *Phys. Rev. B* **1994**, *50*, 17953.
(68) Kresse, G.; Joubert, D. *Phys. Rev. B* **1999**, *59*, 1758.
(69) Monkhorst, H. J.; Pack, J. D. *Phys. Rev. B* **1976**, *13*, 5188.
(70) Duclos, S. J.; Vohra, Y. K.; Ruoff, A. L.; Jayaraman, A.; Espinosa, G. P. *Phys. Rev. B* **1998**, *38*, 7755.
(71) Gerward, L.; Olsen, J. S. *Powder Diffr.* **1993**, *8*, 127.
(72) Chen, Y.; Hu, P.; Lee, M. H.; Wang, H. *Surf. Sci.* **2008**, *602*, 1736.
(73) Illas, F.; Moreira, I. de, P. R.; Bofill, J. M.; Filatov, M. *Phys. Rev. B* **2004**, *70*, 132414.
(74) Wilson, E. L.; Grau-Crespo, R.; Pang, C. L.; Cabailh, G.; Chen, Q.; Purton, J. A.; Catlow, C. R. A.; Brown, W. A.; de Leeuw, N. H.; Thornton, G. *J. Phys. Chem. C* **2008**, *112*, 10918.
(75) Zhang, Ch.; Michaelides, A.; King, D. A.; Jenkins, S. J. *J. Chem. Phys.* **2008**, *129*, 194708.
(76) Lu, J.-L.; Gao, H. -J.; Shaikhutdinov, S.; Freund, H.-J. *Surf. Sci.* **2006**, *600*, 5005.
(77) Lu, J.-L.; Gao, H. -J.; Shaikhutdinov, S.; Freund, H.-J. *Catal. Lett.* **2007**, *114*, 8.

JP8094352